

Article

Design, synthesis and testing of potent, selective hepsin inhibitors via application of an automated closed-loop optimization platform

Shishir M Pant, Amanda Mukonoweshuro, Bimbisar Desai, Manoj K Ramjee, Christopher Nicholas Selway, Gary John Tarver, Adrian G Wright, Kristian Birchall, Timothy M Chapman, Topi A Tervonen, and Juha Klefström

J. Med. Chem., **Just Accepted Manuscript** • DOI: 10.1021/acs.jmedchem.7b01698 • Publication Date (Web): 27 Apr 2018

Downloaded from <http://pubs.acs.org> on April 28, 2018

Just Accepted

"Just Accepted" manuscripts have been peer-reviewed and accepted for publication. They are posted online prior to technical editing, formatting for publication and author proofing. The American Chemical Society provides "Just Accepted" as a service to the research community to expedite the dissemination of scientific material as soon as possible after acceptance. "Just Accepted" manuscripts appear in full in PDF format accompanied by an HTML abstract. "Just Accepted" manuscripts have been fully peer reviewed, but should not be considered the official version of record. They are citable by the Digital Object Identifier (DOI®). "Just Accepted" is an optional service offered to authors. Therefore, the "Just Accepted" Web site may not include all articles that will be published in the journal. After a manuscript is technically edited and formatted, it will be removed from the "Just Accepted" Web site and published as an ASAP article. Note that technical editing may introduce minor changes to the manuscript text and/or graphics which could affect content, and all legal disclaimers and ethical guidelines that apply to the journal pertain. ACS cannot be held responsible for errors or consequences arising from the use of information contained in these "Just Accepted" manuscripts.



ACS Publications

is published by the American Chemical Society, 1155 Sixteenth Street N.W., Washington, DC 20036

Published by American Chemical Society. Copyright © American Chemical Society. However, no copyright claim is made to original U.S. Government works, or works produced by employees of any Commonwealth realm Crown government in the course of their duties.

Design, synthesis and testing of potent, selective hepsin inhibitors via application of an automated closed-loop optimization platform

Shishir M. Pant^{§#}, Amanda Mukonoweshuro^{†a}, Bimbisar Desai^{†b}, Manoj K. Ramjee^{†*}, Christopher N. Selway[†], Gary J. Tarver^{†c}, Adrian G. Wright[†], Kristian Birchall[‡], Timothy M. Chapman^{‡*}, Topi A. Tervonen^{§#}, Juha Klefström^{§#*}

[†] Cyclofluidic Ltd, Biopark, Broadwater Road, Welwyn Garden City, AL7 3AX, UK, +44 (0)1707 358673

^a current address: Charles River Laboratories International Inc., Chesterford Research Park, Little Chesterford, Cambridge, CB10 1XL, UK

^b current address: Virginia Commonwealth University - School Of Engineering, 601 W Main St #331, Richmond, VA 23220, USA

^c current address: New Path Molecular Research, Babraham Research Campus, Cambridge, CB22 3AT, UK

[‡] LifeArc, Accelerator Building, Open Innovation Campus, Stevenage, SG1 2FX, UK, +44 (0)20 7391 2700

[§] Cancer Cell Circuitry Laboratory, Research Programs Unit / Translational Cancer Biology & Medicum, University of Helsinki, P.O. Box 63 (Street address: Haartmaninkatu 8), 00014 University of Helsinki, Finland

ABSTRACT: Hepsin is a membrane-anchored serine protease whose role in hepatocyte growth factor (HGF) signalling and epithelial integrity makes it a target of therapeutic interest in carcinogenesis and metastasis. Using an integrated design, synthesis and screening platform we were able to rapidly develop potent and selective inhibitors of hepsin. In progressing from the initial hit **7** to compound **53**, the IC₅₀ value against hepsin was improved from ~1 μ M to 22 nM and the selectivity over urokinase-type plasminogen activator (uPA) was increased from 30-fold to >6000-fold. Subsequent *in vitro* ADMET profiling and cellular studies confirmed that the leading compounds are useful tools for interrogating the role of hepsin in breast tumorigenesis.

INTRODUCTION

Hepsin is a type II transmembrane serine protease with a chymotrypsin-like serine protease domain containing the catalytic triad of His, Asp and Ser residues.¹ It is frequently overexpressed in prostate, ovarian, renal and breast cancers²⁻⁸ and *in vitro* and *in vivo* studies have revealed the functional role of hepsin in tumour progression and metastasis.^{3,8-10} The prevalence and tumorigenic potential of hepsin in epithelial cancers and its location on the cell surface makes it an accessible cancer therapy target.

Several classes of inhibitors ranging from small molecules, peptides and antibodies have been developed against hepsin.¹¹⁻¹⁶ However, poor understanding of the actions of hepsin in the transformation process has made it difficult to establish a causality between pharmacological inhibition of hepsin activity and reversal of cancerous phenotype *in vitro*. Recent findings suggest that deregulated hepsin has two major oncogenic activities: firstly, hepsin induces processing of several cancer critical growth factors including pro-hepatocyte growth factor (pro-HGF) and pro-macrophage stimulating protein (pro-MSP) into their active forms, leading to activation of tyrosine

kinase receptors mesenchymal epithelial transition factor (MET) and recepteur d'origine nantais (RON).¹⁷⁻²⁰ Secondly, our results with animal tumour models and an inducible form of hepsin suggest an important role for hepsin in disruption of epithelial cohesion junctions, which include desmosomes and hemidesmosomes.^{3,4} These defects will lead to loss of epithelial integrity, which promotes tumour invasion and metastasis.²¹ In a recent study, we identified a urokinase-type plasminogen activator (uPA) inhibitor WX-UK1^{22,23} as a small molecule able to inhibit hepsin activity at low micromolar concentration, prevent hepsin induction-dependent desmosome and hemidesmosome defects and restrain hepsin-induced activation of HGF.³ However, WX-UK1 is a relatively weak hepsin inhibitor ($IC_{50} \sim 3 \mu M$) and exhibits poor selectivity which limits its utility as a molecular tool to study the oncogenic role of hepsin.

Here we set out to identify novel sub-micromolar potency hepsin inhibitors with improved selectivity profiles that would be capable of suppressing both axes of oncogenic hepsin function: growth factor activation and damage to cell junctions. In order to accelerate the generation of new lead molecules, we utilised an integrated design, synthesis and screening platform developed by Cyclofluidic. The small molecule lead generation cycle involves iterative molecular design, chemical synthesis, biological assay and data analysis steps, which feeds into the next cycle. Using conventional processes each cycle may take one or more weeks leading to extended timelines for lead generation, whereas the Cyclofluidic platform dramatically reduces the cycle time to a period of one to two hours and enables rapid and automated lead generation. A comprehensive description of the platform has been published,²⁴ but for this work it was configured as shown (Fig. 1) with integrated reactant handler, flow chemistry system, LC/MS/ELSD analytics and on-line biological assays for hepsin and uPA, and an on-line Chromatographic Hydrophobicity Index (CHI) LogD assay.²⁵ We report here the application of the platform to the identification of potent

hepsin inhibitors, which are able to prevent deregulated hepsin-dependent induction of growth factor signalling and disruption of cell-cell junctions and therefore serve as valuable tools in further probing the role of hepsin.

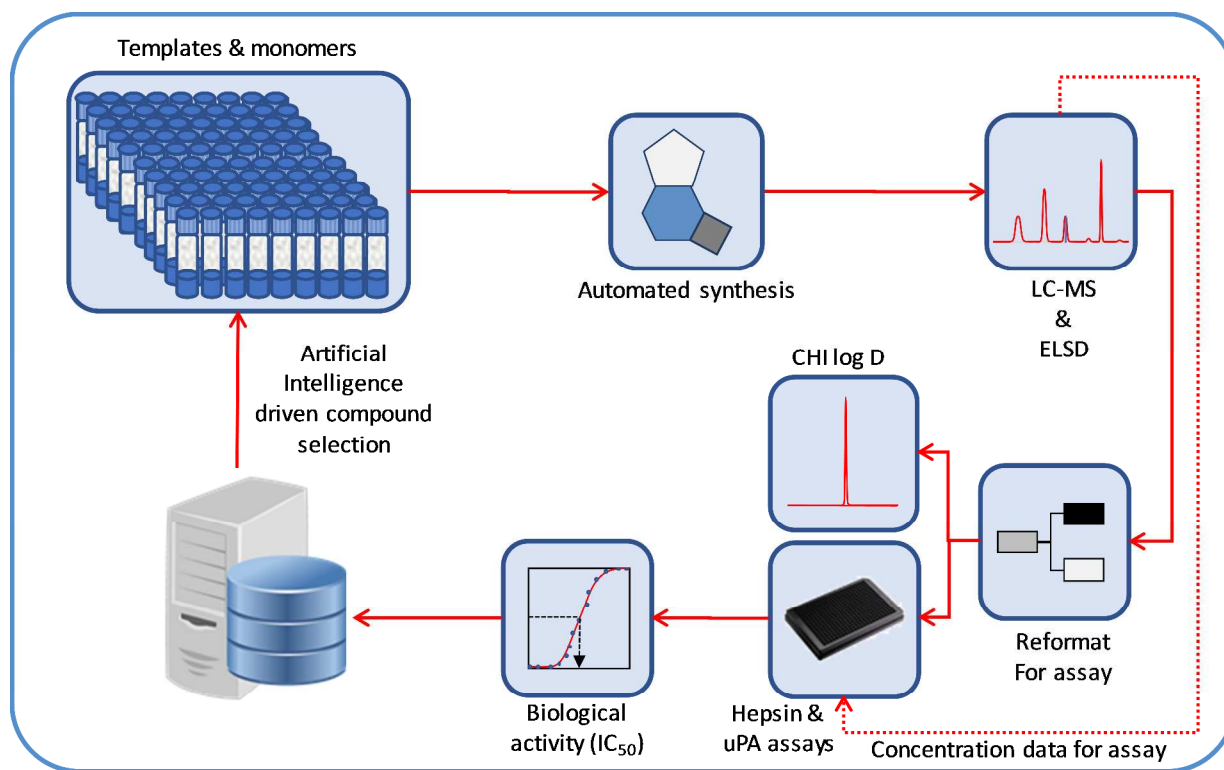
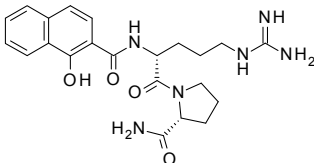
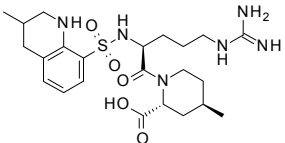
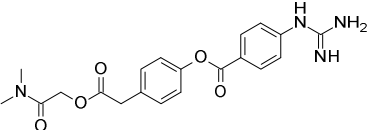
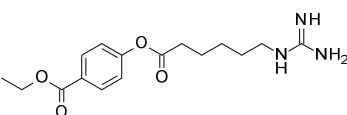
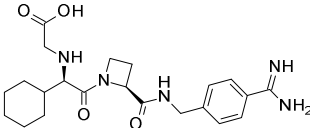
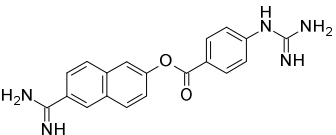
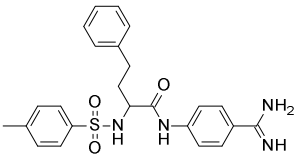
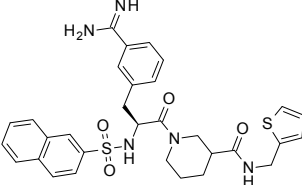


Figure 1. Schematic of the integrated synthesis and screening platform.

RESULTS AND DISCUSSION

Hit Identification. Hepsin shows a strong preference for an arginine residue at the P1 position of its substrates,^{17,26} therefore a series of fourteen commercially available amidine and guanidine-based inhibitors were assayed against hepsin (Table 1). uPA was selected as our initial counterscreen as we sought to identify a starting point which did not display the uPA inhibition exhibited by WX-UK1 (compound **13**).

Table 1. Hepsin screening results for a set of commercially available amidine and guanidine derivatives with uPA counterscreen

Compound Number	Structure	Hepsin IC ₅₀ (μM)	uPA IC ₅₀ (μM)
1		>10	ND
2		>10	ND
3		0.029	ND
4		0.383	ND
5		4.02	ND
6		0.005	ND
7		1.13	>10
8		0.676	2.43

Compound Number	Structure	Hepsin IC ₅₀ (μM)	uPA IC ₅₀ (μM)
9		4.46	ND
10		6.55	>10 ^a
11		0.272	0.484
12		6.19	ND
13		3.35	0.285
14		3.14	>10

^a Literature value²⁷

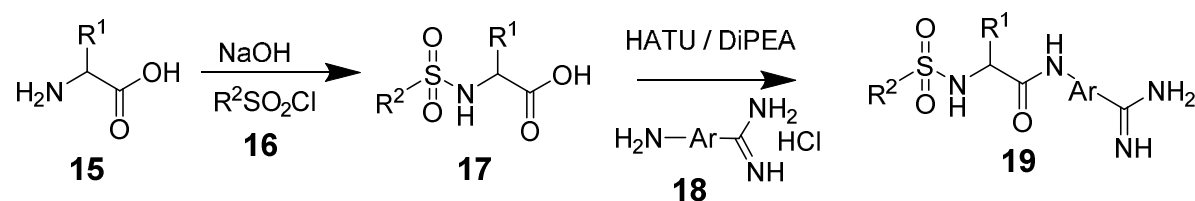
Two compounds, Camostat²⁸ **3** and Nafamostat²⁹ **6** exhibited apparent potent inhibition, however it has been reported³⁰ that this class of compound act as slow tight-binding substrates and exhibit apparent inhibition by stabilising the acyl-enzyme intermediate. This was not the desired mode of action for a selective hepsin inhibitor and these compounds were not considered further.

Compounds **4** and **11** were also not considered structurally attractive starting points; the next most potent compounds **7**^{31,32} and **8**³³ were of more interest and their potency was confirmed in the assay. From these two, compound **7** provided a moderate level of potency, good selectivity for hepsin over uPA and considerable scope for structural modification; it was therefore selected as a suitable starting point for SAR exploration with the goal of optimizing hepsin potency alongside selectivity against uPA.

General Chemistry Methods. General methods for the batch and flow synthesis of compound **7** analogs are described below, and full details are provided in the supporting information.

Batch Method: Initial batch synthesis of compound **7** analogs³⁴ of general structure **19** was undertaken as illustrated in Scheme 1.

Scheme 1. Batch-based synthetic route to compound **7** analogs

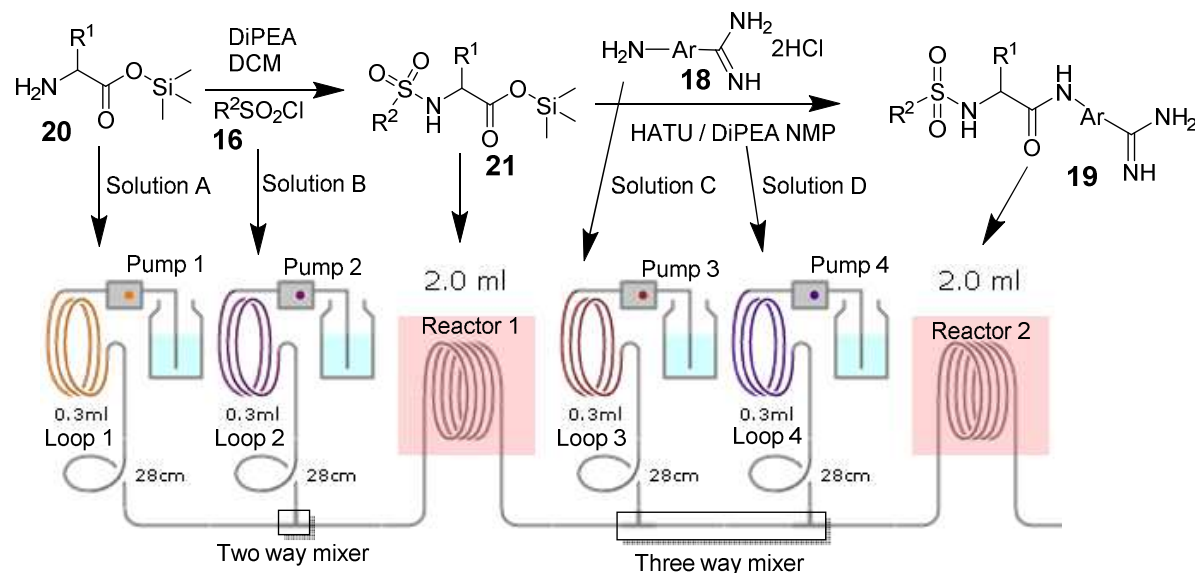


Reaction of a sulfonyl chloride **16** with an amino acid **15** in aqueous sodium hydroxide, followed by acidification and extractive work up gave an intermediate sulfonamide **17**. The crude intermediate was reacted with an aminoamidinium **18** using 2-(3H-[1,2,3]triazolo[4,5-b]pyridin-3-yl)-1,1,3,3-tetramethylisouronium hexafluorophosphate (HATU) as the coupling agent to give the product **19**. Regioselective reaction at the aniline moiety rather than the amidine of **18** was ensured through the protection of the very basic amidine as a hydrochloride salt, readily achieved

through the use of *N*-ethyl-*N*-isopropylpropan-2-amine (DIPEA) as reaction base. The desired product was purified by reverse phase HPLC.

Flow Method: In order to successfully prepare a range of analogues utilising the CyclOps platform a flow chemistry method was developed based on the batch synthesis (Scheme 2). Amino acids are inherently insoluble in solvents more suited to flow synthesis; therefore the use of preformed trimethyl silyl esters of the acids addressed both the insolubility of the amino acids and offered the advantage of transient protection of the carboxylic acid functionality. No formal de-protection step was required as the ester proved labile under the reaction conditions.

Scheme 2. Flow-based synthetic route to compound 7 analogs



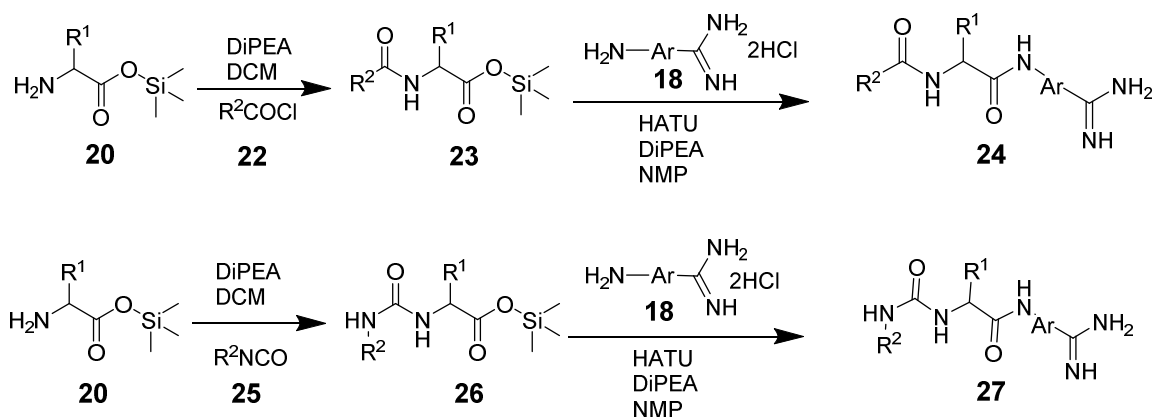
Stock solutions **A** of silylated amino acid trimethylsilyl esters **20** were pre-prepared in batch by reaction of an amino acid **15** with chlorotrimethylsilane and DIPEA in dichloromethane under microwave conditions for 10 to 20 min at 100°C. They were used without further purification by reaction in a flow reactor with stock solution **B** of a sulfonyl chloride **16** in dichloromethane at

60°C and a total flow rate of 100 μ L/min. After 20 min the intermediate sulfonamide product **21** eluted from reactor 1. It was immediately mixed under flow conditions with a stock solution **C** of amidine dihydrochloride **18** in NMP containing 1 equivalent of DIPEA and stock solution **D** of HATU and DIPEA in NMP. The reaction mixture was heated at 100°C in reactor 2 for 10 min at a total flow rate of 200 μ L/min to provide a solution of the final product **19**, which was purified by HPLC prior to screening.

The regioselective formation of the desired amide in the presence of the amidine was again achieved by ensuring the more basic amidine was protected as the hydrochloride salt throughout the coupling reaction and the two steps could be seamlessly telescoped together to enable the flow synthesis of a range of structures. All flow based synthetic methods were undertaken using the Vapourtec³⁵ R4 chemistry apparatus.

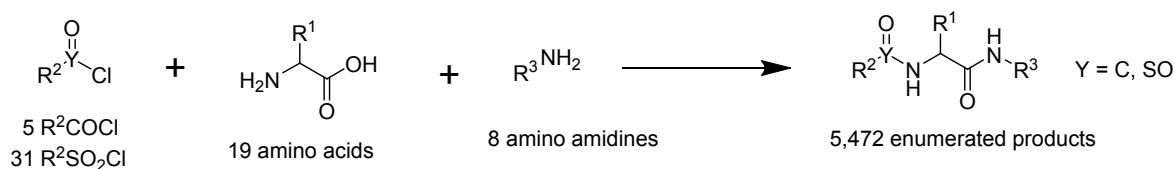
The scope of the reaction described above was extended to cover synthesis of amide analogs **23** and **24** and also urea analogs **26** and **27**, using acid chlorides **22** and isocyanates **25**, respectively, instead of the sulfonyl chloride in step 1, Scheme 3. In general, the relevant acid chloride or urea building blocks were used as direct substitutes of the sulfonyl chlorides.

Scheme 3. Two-step amide and urea formation followed by amidoamidine formation from amino acid trimethylsilyl esters in flow



Platform SAR Strategy. The integrated platform offers an efficient and effective means to rapidly explore the SAR of a defined area of virtual chemistry space. Compound **7** can be readily disconnected to three reaction components, each readily accessible through commercial suppliers. A subset of available reactants was selected which when enumerated represent the virtual chemistry space for the platform SAR generation (Scheme 4).

Scheme 4. Representation of the virtual chemistry space for platform SAR generation



This set of 63 reactants (see Supporting Information for structures) represented a chemistry space of 5,472 virtual molecules for initial exploration on the integrated platform. This initial set of reactants was chosen based on commercial availability, synthetic compatibility and diversity. Exploration of the SAR represented by this virtual chemical space was undertaken using a multiparameter optimization method to select the predicted most potent compounds against the

primary target hepsin and with the best predicted selectivity over uPA. This multiparameter objective was defined as maximising the predicted potency against hepsin (*i.e.* lower IC₅₀ values) and minimising the predicted potency for uPA (*i.e.* higher IC₅₀ values) and is referred to as the platform objective.

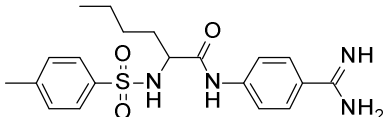
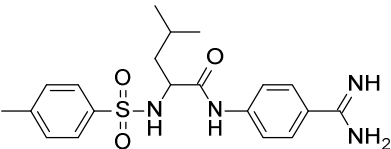
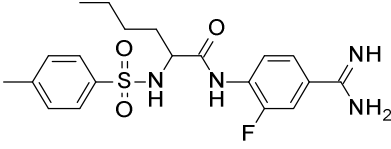
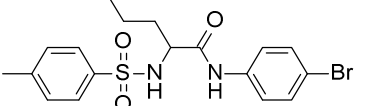
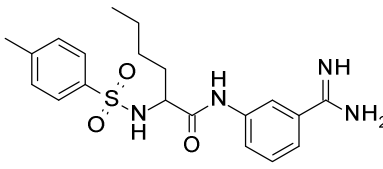
In order to maximise the exploration of the selected chemical reactants whilst seeking selective and potent structures, the initial strategy chosen was Best Objective Under Sampled (BOUS). At the start of a platform experiment the algorithm predicts IC₅₀ values based on the prior knowledge data set (the results of the commercial compound screen were initially used for this). The desirability of each compound is then determined using the platform objective.

To determine the order of synthesis for the platform for each eligible virtual product, the total is calculated of the number of times the constituting reactants have been used previously. The compounds with the lowest total previous usage are considered to be under sampled, and synthesizing compounds from this pool ensures all reactants are sampled as equally as possible.

At the end of each complete synthesis and screen cycle the prior knowledge data set is updated to include the new inhibition values, the selection algorithm is repeated and the next compound for synthesis and screening is selected for the platform. Each closed loop cycle took approximately 90 minutes on the platform and the process is fully automated (*i.e.* subsequent cycles continue without any intervention). Following a set of automated experiments the developing SAR is evaluated and a new set of experiments devised that may include changes in the reactant sets used on the platform as well as the optimization strategy. In this work a series of five distinct sets of automated experiments were carried out, and the results from these are described below as Platform Experiments 1 to 5.

Platform Experiments 1 – Best Objective Under-Sampled Experiment. An initial set of 24 closed-loop synthesis and screening experiments, using the BOUS strategy to select from within the 5,472 virtual set, quickly established that compounds derived from 4-aminobenzamidine showed the best activity against hepsin and the other seven aminoamidines in the reactants set were only weakly active in the examples made. A number of chemical reactivity trends were also established, the main ones being that aromatic sulfonyl chlorides worked well, but in general aliphatic sulfonyl chlorides failed to react, and hindered amino acids usually failed to react too. In addition a number of reactants were found to be insoluble in the required solvents. Based on reactivity and this initial SAR, a number of reactants were removed from the set and the experiment was continued with a subset of thirteen amino acids, thirty-two sulfonyl/acid chlorides and five aminoamidines. A final total of sixty-three synthesis to screen cycles using BOUS were attempted and forty-four gave reliable SAR data (70%) (see Supporting Information for structures). Three compounds **28**, **29** and **30** gave hepsin IC₅₀ values below 1 μ M, with uPA activity generally around ten-fold weaker (Table 2). The CHI LogD in this series was also improved compared to **7** (CHI LogD = 4.2). It was apparent that the highest hepsin inhibition was observed in 4-methylbenzene sulfonamide derivatives of small aliphatic amino acids such as leucine and norleucine, combined with para-substituted aminobenzamidines. The matched pair **28** and **31** confirmed the importance of the amidine to binding; replacing it with a bromine led to a large loss in activity.

Table 2. Selected results from Best Objective Under-Sampled experiment and aminoamidine scan

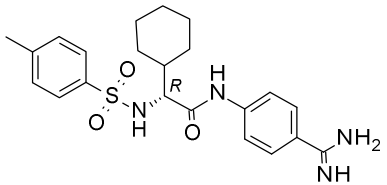
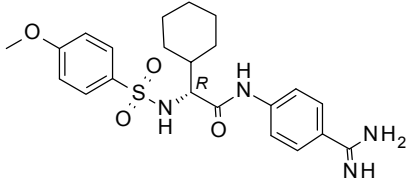
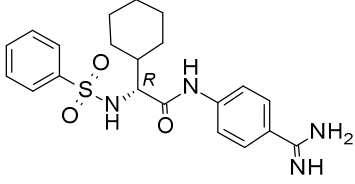
Structure	Compound Number	Hepsin IC ₅₀ (μM)	uPA IC ₅₀ (μM)	Selectivity ratio	CHI LogD
	28	0.5 0.9 ^a	5 3 ^a	10 3	1.2
	29	0.9 0.6 ^a	11 20 ^a	12 33	1.2
	30	0.9	8	9	1.4
	31	58	58	1	NA ^b
	32	73	19	0.26	1.1

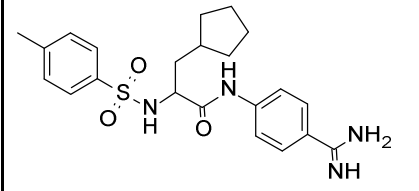
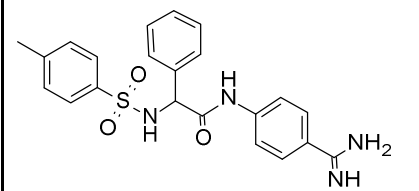
^a Repeat synthesis and screening data; ^b Data not available.

Platform Experiments 2 – Aminoamidine Scan. To further examine the effect of changing the aminoamidine component an additional five compounds were synthesized and screened using the platform, keeping 4-methylbenzene sulfonyl chloride and norleucine constant while varying the aminoamidine moiety. The results confirmed the SAR in this region is very tight: for example changing from the *para*- to the *meta*-aminobenzamidine derivative **32** (Table 2) resulted in a significant loss of activity, as did replacing the amidine with a nitrile or N-methylation at the amide (data not shown).

Platform Experiments 3 – Chase Objective Strategy. Based on the SAR obtained up to this point, the original set of 5,472 virtual compounds was refined down to a much smaller set of 297 virtual compounds derived from 27 sulfonylating/acylating agents, 11 amino acids and 1 aminoamidine. The new chemical space was efficiently explored using a Chase Objective strategy to run multiple closed-loop synthesis and screening experiments, with 80% success rate overall. The highest hepsin activity was seen in products derived from aliphatic amino acids; a summary of these are shown Table 3. In particular, the product **33** derived from (*R*)-cyclohexylglycine (Table 3) gave a hepsin IC₅₀ of 33 nM and greater than one hundred-fold selectivity when initially run on the platform, and similar values on repeat off-line screening of the collected fraction. CHI LogD values are also within a generally acceptable range, although the properties are strongly influenced by the highly basic amidine moiety.

Table 3. Selected results following Chase Objective experiments

Structure	Compound Number	Hepsin IC ₅₀ (μM)	uPA IC ₅₀ (μM)	Selectivity ratio	CHI LogD
	33	0.033 0.070 ^a 0.038 ^b	4.4 >10 ^a >41 ^b	133 >142 >1000	1.3
	34	0.3	12	40	1.3
	35	1.1	22	20	1.2

Structure	Compound Number	Hepsin IC ₅₀ (μM)	uPA IC ₅₀ (μM)	Selectivity ratio	CHI LogD
	36	0.7	16	23	1.5
	37^b	0.25	60	240	0.9

^a Manual screen of platform synthesized sample; ^b Off-line synthesis and manual screen.

To confirm this result, **33** was synthesized off-line and assayed manually (Figure 2). The hepsin IC₅₀ was 38 nM and uPA IC₅₀ was >41 μM, indicating >1000-fold selectivity.

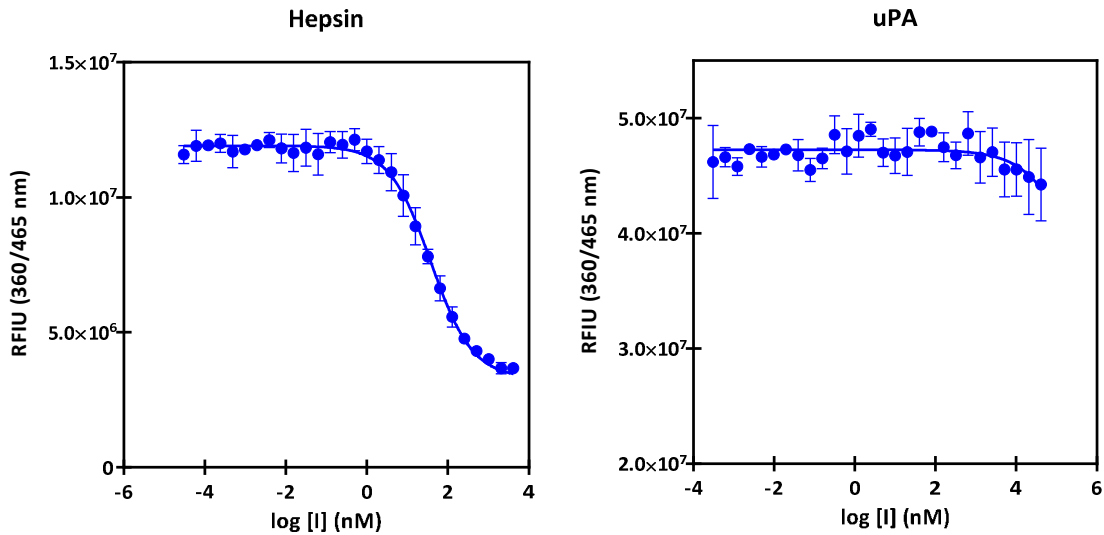


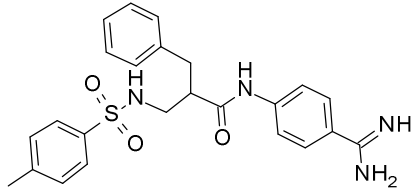
Figure 2. Hepsin and uPA IC₅₀ curves for compound **33**.

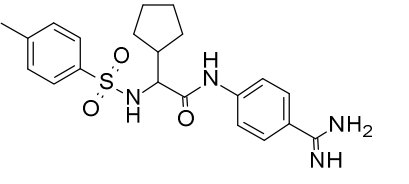
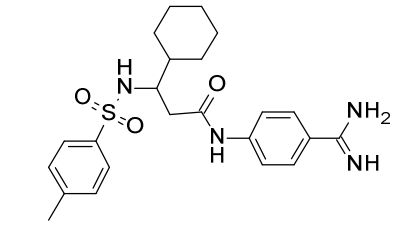
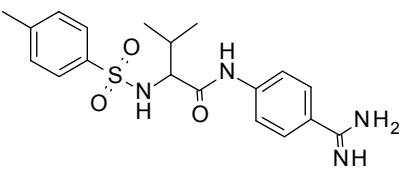
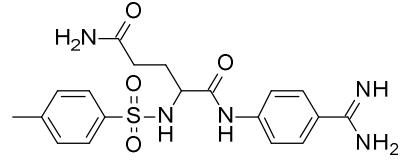
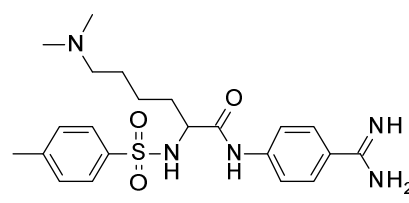
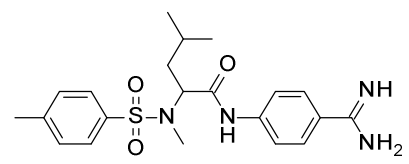
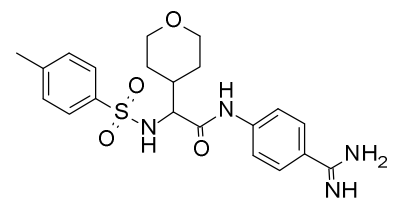
The synthesis of the racemic phenylglycine derivative **37** (Table 3) failed on the platform, so it was synthesized off-line and assayed manually to compare activity of the phenyl and cyclohexyl matched pair. The hepsin IC₅₀ was 250 nM and uPA IC₅₀ was 60 μM, indicating ~240-fold

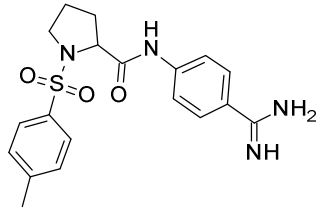
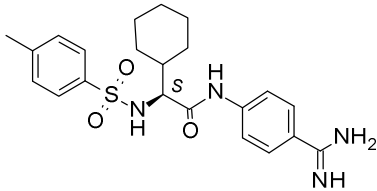
selectivity, but overall about 7-fold weaker against hepsin than the (*R*)-cyclohexylglycine compound **33**. However, later evaluation of the (*R*)-phenylglycine derivative **53** showed it to have similar potency to **33**.

Platform Experiments 4 – Amino Acid Scan. To further examine the effect of changing the amino acid component, the synthesis and screening of a series of nine compounds was attempted on the platform with 4-methylbenzene sulfonyl chloride and 4-aminobenzamidine kept constant while the amino acid was varied. Seven of these were successfully completed and the results, shown in Table 4, indicated that the cyclopentyl derivative **39** had good selectivity and reasonable hepsin activity although it was weaker than the cyclohexyl analogue **33** and phenyl analogue **37**. It was also clear that β -amino acid derivatives such as **38** and **40** were generally weaker than α -amino acids. Interestingly the tetrahydropyranylglycine derivative **45** was ~30-fold weaker than compound **33** indicating that polarity was not well tolerated at this position. Unfortunately the syntheses of **42** from glutamine and **43** from dimethyl lysine failed, so the tolerance for other polar side chains could not be tested.

Table 4. Hepsin and uPA activity data from variation of the amino acid

Structure	Compound Number	Hepsin IC ₅₀ (μM)	uPA IC ₅₀ (μM)	Selectivity ratio	CHI LogD
	38	3	1	0.3	1.6

Structure	Compound Number	Hepsin IC ₅₀ (μM)	uPA IC ₅₀ (μM)	Selectivity ratio	CHI LogD
	39	0.86	64	74	0.4
	40	11	68	6	1.4
	41	1.8	7.2	4	0.8
	42 ^a	NR	NR		
	43 ^a	NR	NR		
	44	>19	24	<1	1.8
	45	1.4	>19	>13	0.4

Structure	Compound Number	Hepsin IC ₅₀ (μM)	uPA IC ₅₀ (μM)	Selectivity ratio	CHI LogD
	46	3 1.5	28 5.3	9 3	0.5
	47	0.22 ^b			1.3

^a Synthesis failed; ^b Manual synthesis and screening.

In addition, the (*S*)-cyclohexylglycine derivative **47** (Table 4) was synthesized manually to provide a comparison of the hepsin activity of the two enantiomers (Figure 3). The (*R*)-cyclohexylglycine derivative **33** was measured three times in sequential experiments and was slightly weaker in this comparison than previously measured but the data suggests the (*S*)-enantiomer is 2- to 3-fold weaker, but note the enantiomeric purity of the two samples has not been measured directly.

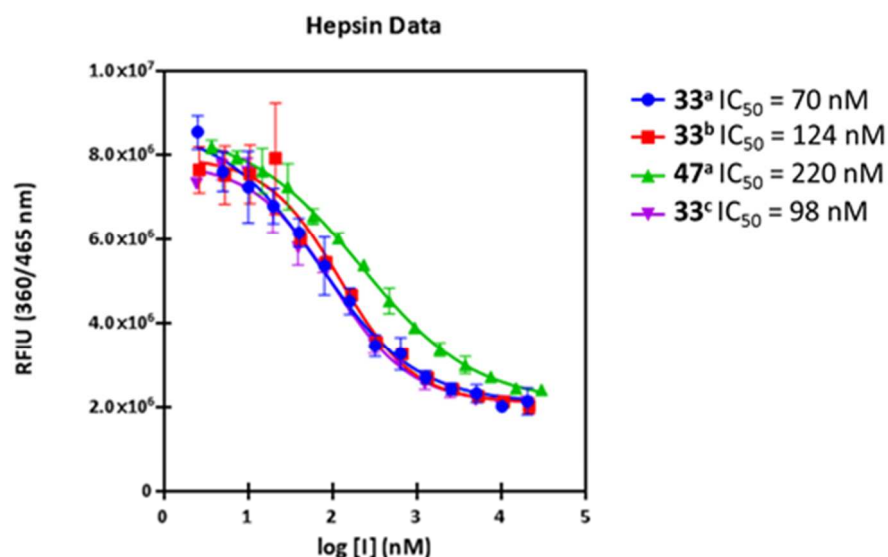
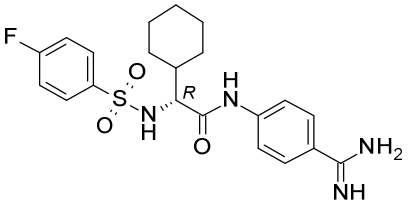
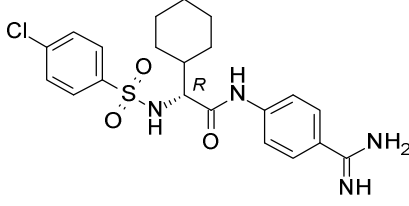
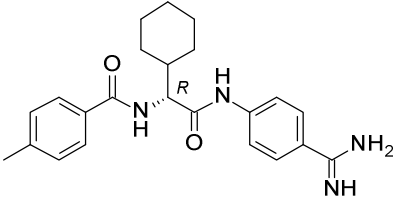
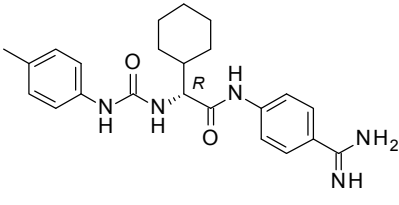
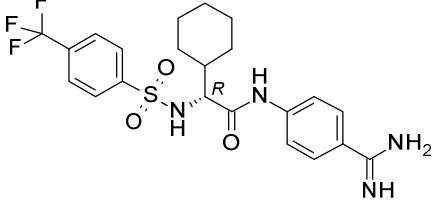


Figure 3. Hepsin activity comparison of the (*S*) and (*R*) enantiomers of the cyclohexylglycine derivatives. ^a Platform used to purify and collect sample with manual off-line screening; ^b Repeat of 'a'; ^c Pure solid sample with manual screening.

Platform Experiments 5 – Extending the Chemical Space. To further explore the SAR a new medicinal chemistry design was undertaken and a set of 186 virtual compounds, derived from 31 sulfonylating / acylating agents, 6 amino acids and a single aminoamidine (4-aminobenzamidine), was defined. The selection of the building blocks forming this virtual space was made based on an evaluation of the existing SAR, commercial availability, synthetic tractability and also the desire to extend into untapped areas, for example the acylating reagents included some isocyanates to yield urea derivatives. The full set of reactants is shown in the Supporting Information. The platform was run for 22 synthesis-to-screen cycles using BOUS. It was immediately apparent that only the cyclohexylglycine and cyclopentylglycine derivatives showed good hepsin activity and selectivity. Hence a Chase Objective experiment was set up with only cyclohexylglycine and cyclopentylglycine amino acids along with the remaining sulfonylating / acylating agents. A further 21 loops were run in this mode to extend the SAR. The analogs derived from *p*-fluorobenzenesulfonyl chloride **48** and *p*-chlorobenzenesulfonyl chloride **49** showed some of the best activity from this set against hepsin and good selectivity over uPA (Table 5). The matched cyclohexylglycine triplet of the sulfonamide **33**, amide **50** and urea **51** show the activity sequence sulfonamide >>> urea > amide. The larger *p*-trifluoromethylphenylsulfonamide **52** showed reduced potency versus its methyl analogue **33**.

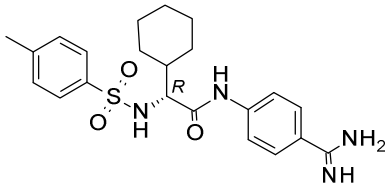
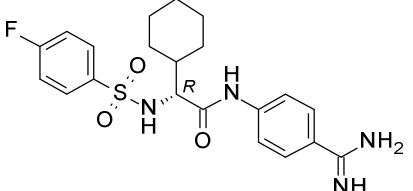
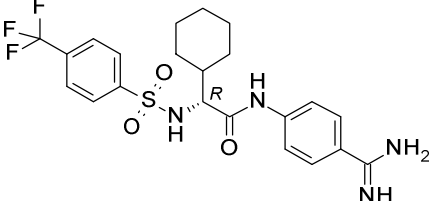
Table 5. Examples of active compounds and matched pairs synthesized on the platform

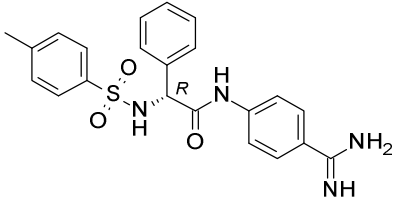
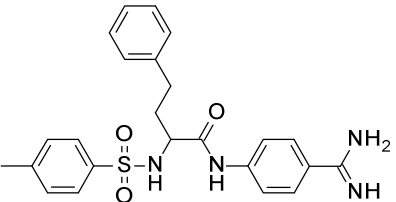
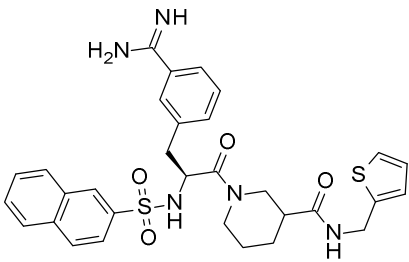
Structure	Compound Number	Hepsin IC ₅₀ (μM)	uPA IC ₅₀ (μM)	Selectivity ratio	CHI LogD
	48	0.09	>14	>155	NA
	49	0.10	18	180	1.5
	50	5.0	24.5	5	1.7
	51	2	43	22	1.5
	52	0.68	4.7	7	1.7

Off-line synthesis of samples for further analysis and testing. Four inhibitors spanning a range of potencies were synthesized off-line in batch mode and assayed manually against hepsin and uPA (alongside **7** and **8** as standards) in order to allow comparison with the results obtained on the

platform and to generate sufficient solid sample for further testing. This group included the product derived from (*R*)-phenylglycine, compound **53** (Table 6). The IC₅₀ values are shown in Table 6 and the initial IC₅₀ curves are shown in Figure 4. The most potent compound, the phenylglycine derivative **53** initially showed a potency of 4 nM, but the curve was not a complete sigmoidal shape at the lower concentration, so a second assay covering lower concentrations was run for this compound (Figure 5). The curve showed a better shape and the potency was 22 nM against hepsin with >6000 fold selectivity over uPA. The (*R*)-cyclohexylglycine derivative **33** was slightly weaker than **53** but still shows excellent potency and selectivity.

Table 6. Hepsin and uPA activity of four selected compounds synthesized off-platform with two original hit compounds included as standards

Structure	Compound Number	Hepsin IC ₅₀ (μM)	uPA IC ₅₀ (μM)	Selectivity
	33	0.056	1946	34000
	48	0.19	280	1450
	52	0.85	>1946	>2300

Structure	Compound Number	Hepsin IC ₅₀ (μM)	uPA IC ₅₀ (μM)	Selectivity
	53	0.022	140	6363
	7	0.87	26	30
	8	0.33	6	18

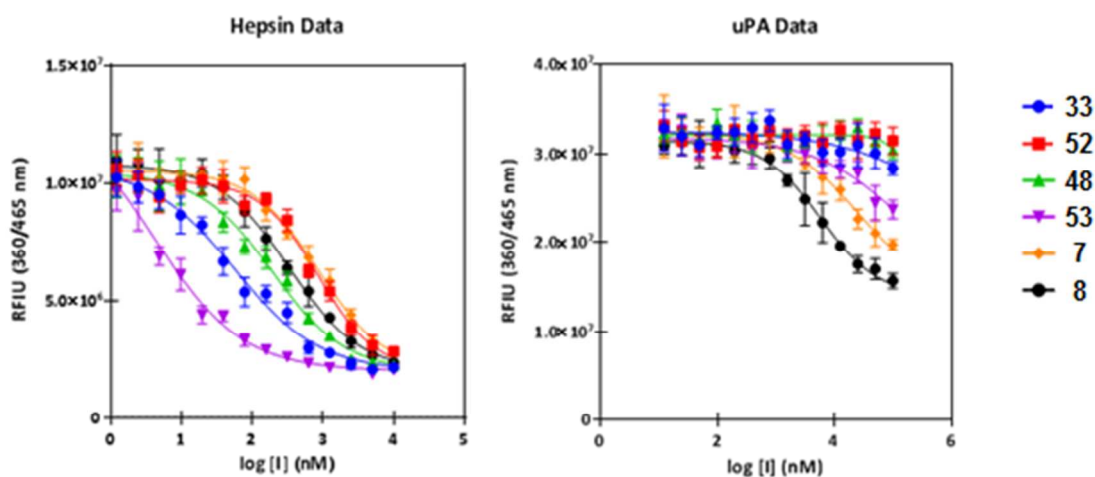


Figure 4. Hepsin and uPA IC₅₀ curves for four compounds synthesized off-platform with two original hit compounds as standards

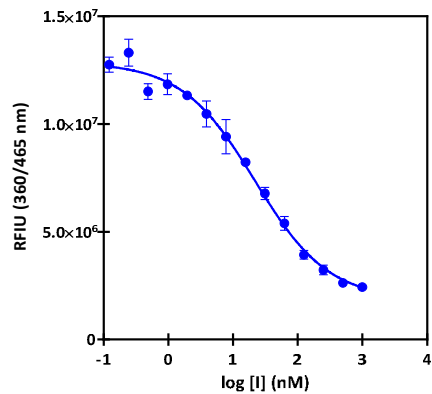


Figure 5. IC₅₀ curve for compound 53 against hepsin.

Selectivity & *in vitro* ADMET profiling. The leading compounds were profiled against a panel of 10 serine proteases to assess their broader selectivity (Table 7). The three compounds tested displayed similar selectivity profiles, with the most potent hepsin inhibitor **53** exhibiting 54% and 34% inhibition of trypsin and plasma kallikrein respectively at 1 μ M inhibitor concentration.

Table 7. Serine protease selectivity profiling of key compounds; values given are % inhibition (mean of 2 experiments) at compound concentrations of 1 μ M and 10 μ M

Serine Protease, % inhibition at given compound concentration	33		48		53	
	1 μ M	10 μ M	1 μ M	10 μ M	1 μ M	10 μ M
Thrombin	11	12	NI	10	NI	44
Chymase	NI	NI	NI	NI	NI	NI
Elastase	NI	NI	NI	NI	NI	NI
Cathepsin G	NI	NI	NI	NI	NI	NI
Dipeptidyl peptidase	NI	NI	NI	NI	NI	NI
Trypsin	52	98	40	91	27	80

Trypsin	83	96	77	97	54	93
Plasma kallikrein	NI	29	12	34	34	85
ELA2 (Neutrophil Elastase 2)	NI	NI	NI	NI	NI	NI
Matriptase	NI	NI	NI	NI	NI	NI
HGFA	18	22	10	24	16	24
Factor Xa	NI	NI	NI	NI	NI	NI

NI = no significant inhibition observed (<10%)

Compounds **33**, **48** and **53** were also profiled in *in vitro* ADMET assays (Table 8). Due to the influence of the highly basic benzamidine group, all three compounds showed high solubility and no PAMPA permeability; however, given the extracellular location of the protease domain of hepsin, the lack of permeability observed does not limit their application in cell-based assays. Metabolic stability was acceptable in both mouse and human microsomes, with the exception of the low stability of **48** in human microsomes. The compounds showed no cytotoxicity in Hep-G2 cells up to 10 μ M concentration.

Table 8. *In vitro* ADMET profiling of key compounds

Compound number	33	48	53
Kinetic solubility (μ M)	>200	200	>200
MLM $t_{1/2}$ (min)	74	48	108
HLM $t_{1/2}$ (min)	89	16	53
PAMPA P_{app} (nm/s)	0	0	0
Cytotox Hep-G2 viable-50 (μ M)	>10	>10	>10

MCF10A-Indu20-hepsin cell based assay. We employed non-transformed mammary epithelial MCF10A cells expressing doxycycline (Dox) inducible hepsin (MCF10A-Indu20-hepsin) as a

cell-based assay to test whether the key compounds inhibit oncogenic hepsin functions. In this cell system, addition of Dox to the cells induces a level of hepsin protein expression and activity that is comparable to breast tumour cell lines.³ The inducible system for hepsin expression is described in Figure 6 (a-c). Hepsin induction leads to down-modulation of its cognate inhibitor HAI-1, which serves as one readout of oncogenic hepsin activity (Figure 6b).

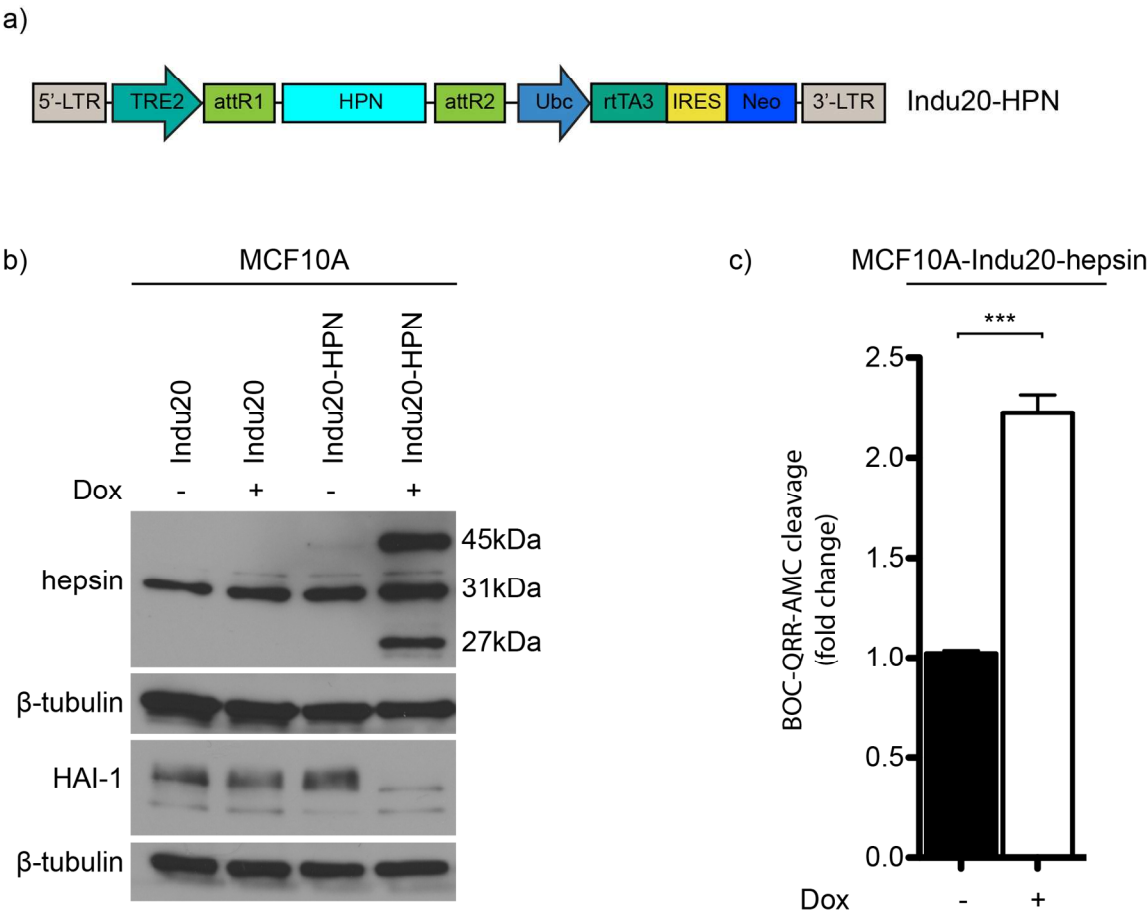


Figure 6. Doxycycline-inducible hepsin expression in non-transformed mammary epithelial MCF10A cells. a) Schematic presentation of pINDUCER20-HPN (Indu20-HPN) vector construct. b) Doxycycline induction of Indu20-HPN in MCF10A (MCF10A-Indu20-hepsin) cells leads to increased expression of processed forms of hepsin and down modulation of HAI-1. c) Dox-

induction leads to increased cleavage of hepsin selective substrate BOC-QRR-AMC. For hepsin induction cells were treated with 100 ng/mL Dox for 24 h. * $p < 0.05$, ** $p < 0.01$, *** $p < 0.001$.

We used the MCF10A-Indu20-hepsin cells to determine the cellular IC_{50} values of the compounds against hepsin using fluorogenic BOC-QRR-AMC peptide as a hepsin selective substrate. All four compounds displayed IC_{50} values in the range of 0.10-3.15 μ M. Compound **53** was the most potent inhibitor of hepsin with an IC_{50} of 0.10 μ M and is therefore significantly more potent than WX-UK1 (IC_{50} 6.49 μ M). Compound **33** and **48** inhibited hepsin with IC_{50} values of 0.99 μ M and 1.29 μ M respectively, while **52** was the least potent inhibitor with an IC_{50} of 3.15 μ M (Figure 7a,b). The proteolytic activity of hepsin is regulated by its cognate inhibitor HAI-1 at the cell surface and oncogenic levels of hepsin lead to enhanced shedding of HAI-1 from the cell membrane, a phenomenon not seen with the overexpression of catalytically inactive hepsin.³ To test whether the compounds were able to prevent the loss of HAI-1, MCF10A-Indu20-hepsin cells were treated with the compounds prior to induction of hepsin with doxycycline. In these experiments, compound **53** prevented the hepsin-induced loss of HAI-1 at 10 μ M concentration. We have previously shown that WX-UK1 inhibits HAI-1 down modulation at 20 μ M concentration. However, neither WX-UK1 nor any of the other compounds was able to efficiently prevent HAI-1 loss at 10 μ M concentration, which is consistent with the superior potency of **53** seen in biochemical and cell based IC_{50} assays (Figure 7c).

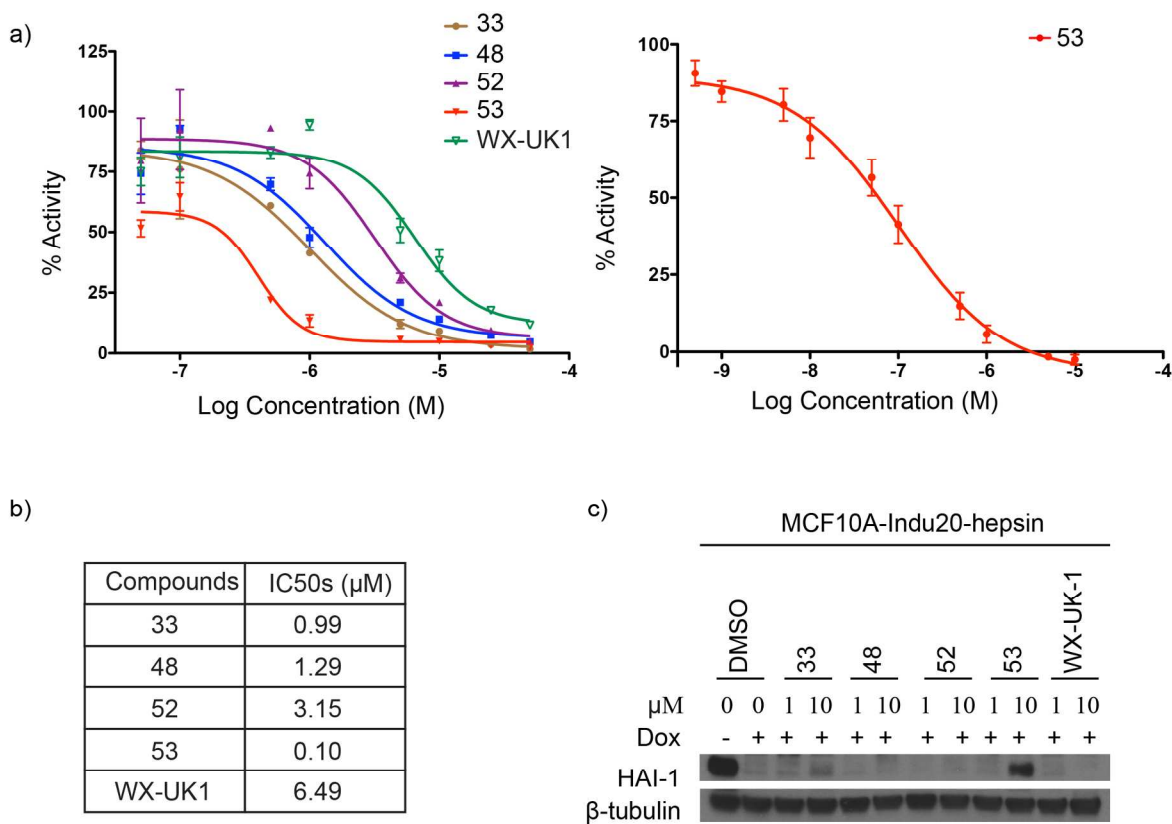


Figure 7. Inhibition of the proteolytic activity of hepsin. a) Determining the IC₅₀ from the cellular dose-response curve. The inhibitory action of compounds **33**, **48**, **52**, **53** and WX-UK1 was measured in MCF10A-Indu20-hepsin cells using BOC-QRR-AMC as a substrate. Due to the higher potency of **53**, the IC₅₀ curve was generated with a broader concentration range. b) IC₅₀ values of the tested compounds. c) Inhibition of hepsin-dependent down-modulation of cellular HAI-1. MCF10A-Indu20-hepsin cells were pre-treated with either DMSO or the compounds for 30 min followed by induction of hepsin with 100 ng/mL doxycycline for 6 h. HAI-1 protein levels were analyzed by immunoblot.

Inhibition of hepsin-dependent activation of HGF/MET signalling pathway. Hepatocyte growth factor is produced in its latent form (Pro-HGF) by mesenchymal cells and requires a

1
2
3 proteolytic cleavage for conversion into active α and β chains.³⁶ Several studies have shown that
4
5
6 hepsin activates Pro-HGF, consequently activating MET receptor tyrosine kinase.^{3,17,37} The
7
8 HGF/MET pathway is associated with poor prognosis and acquired drug resistance in several
9
10
11 cancers.^{38,39} We examined whether the lead compounds inhibit hepsin-mediated processing of
12
13 recombinant human ProHGF (rPro-HGF) by incubating rPro-HGF with recombinant human
14
15 hepsin (rhHPN) in the presence of inhibitors. Compound **53** demonstrated the highest inhibition of
16
17 rPro-HGF activation shown by a decrease in α and β chain processing (Figure 8a). To further
18
19 evaluate the capacity of our compounds to prevent HGF/MET signalling, we induced hepsin with
20
21 Dox in MCF10A-Indu20-hepsin cells and treated them with the inhibitors and rPro-HGF.
22
23 Compound **53** displayed the best potency against HGF/MET activation as demonstrated by the
24
25 decrease in MET phosphorylation (Figure 8b).

26
27
28 We have recently shown that hepsin protein is overexpressed in all major subtypes of breast
29
30 cancer, with the highest frequency of overexpression in triple negative breast cancer (TNBC).³ We
31
32 tested the efficacy of the inhibitors on HGF/MET signalling in a TNBC cell line Hs578T, which
33
34 expresses high levels of proteolytically active hepsin and low levels of HAI-1.³ Treatment of
35
36 Hs578T cells with rPro-HGF led to an increase in MET phosphorylation, which was inhibited by
37
38 all four compounds (Figure 8c). Consistent with our previous results, **53** demonstrated superior
39
40 potency compared to the other compounds (Figure 8c). We confirmed the results with **53** in two
41
42 TNBC cell lines, Hs578T and HCC1937. In these assays, 1 μ M **53** inhibited MET phosphorylation
43
44 similarly to the clinically tested MET inhibitor crizotinib at 100 nM (Figure 8d,e).

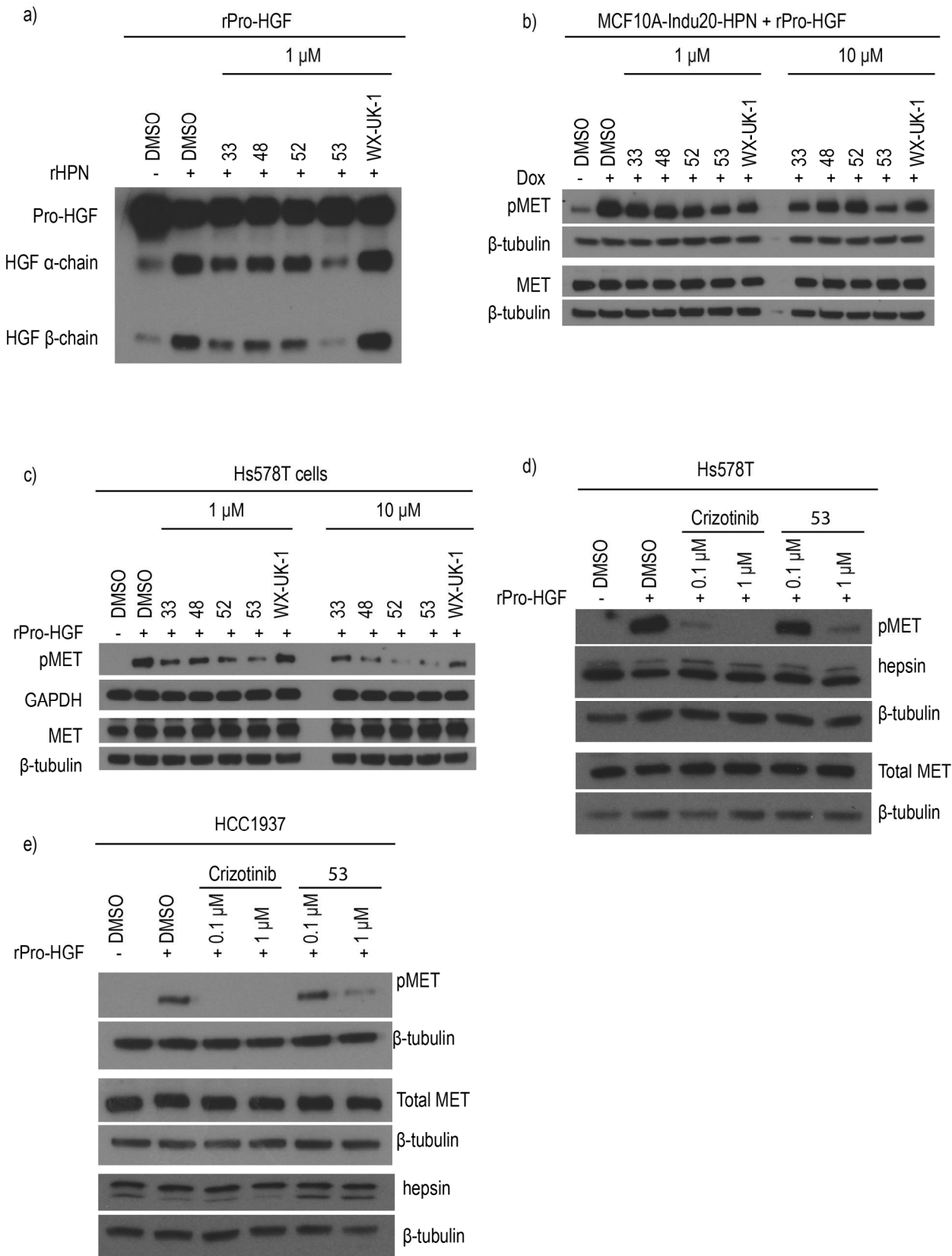


Figure 8. Inhibition of the hepsin mediated activation of HGF/MET-signalling. a) Compound **53** inhibits recombinant human hepsin (rhHPN) mediated processing of recombinant human HGF propeptide (rPro-HGF). rPro-HGF was incubated in the presence of rHPN at 37°C for 30 min together with indicated inhibitors. rPro-HGF processing was analyzed by immunoblotting using antibody recognizing Pro-HGF as well as α and β chains; b,c) Inhibition of hepsin mediated conversion of Pro-HGF into active form. Measured is MET phosphorylation (Tyr1243/1245). In b, Dox-induced MCF10A-Indu20-hepsin cells were treated with DMSO or inhibitors for 30 min followed by addition of 50 ng/mL rPro-HGF. In c, the Hs578T cell line was incubated with DMSO or inhibitors as indicated followed by addition of 50 ng/mL rPro-HGF. Inhibition of the MET pathway activation was analyzed by immunoblotting; d,e) Comparison of MET inhibition by compound **53** and crizotinib in Hs578T and HCC1937 cell lines. Cells were treated as in c).

Prevention of hepsin-mediated loss of desmosomes. Elevated levels of hepsin in tumours contribute to loss of epithelial integrity, which is a defining feature of tumour progression from a local *in situ* tumour to invasive cancer.^{3,4} Hepsin is localized to desmosomal junctions in epithelial cells and high hepsin levels break desmosomes, which are important for cell-cell cohesion.^{3,8} Therefore, the degrading actions of oncogenic hepsin on desmosomes could be defining factors in the process of loss of epithelial integrity during tumorigenesis. Desmogleins are desmosomal cadherins, which show a pericellular network-like staining pattern in non-transformed MCF10A cells. Dox-induction of hepsin results in the loss of desmosomal structures, visualized by loss of desmoglein 2 staining. We explored whether compound **53**, which demonstrated the highest potency against hepsin, would inhibit hepsin-mediated loss of desmosomes. MCF10A-Indu20-

hepsin cells were treated with **53**, WX-UK1 or DMSO for 30 min followed by hepsin induction with Dox. In this setting, **53** but not WX-UK1 was able to alleviate hepsin-mediated desmosomal defect (Figure 9a,b). The results show that hepsin-induced desmosomal damage can be subjected to intervention with small molecule approaches in cell culture.

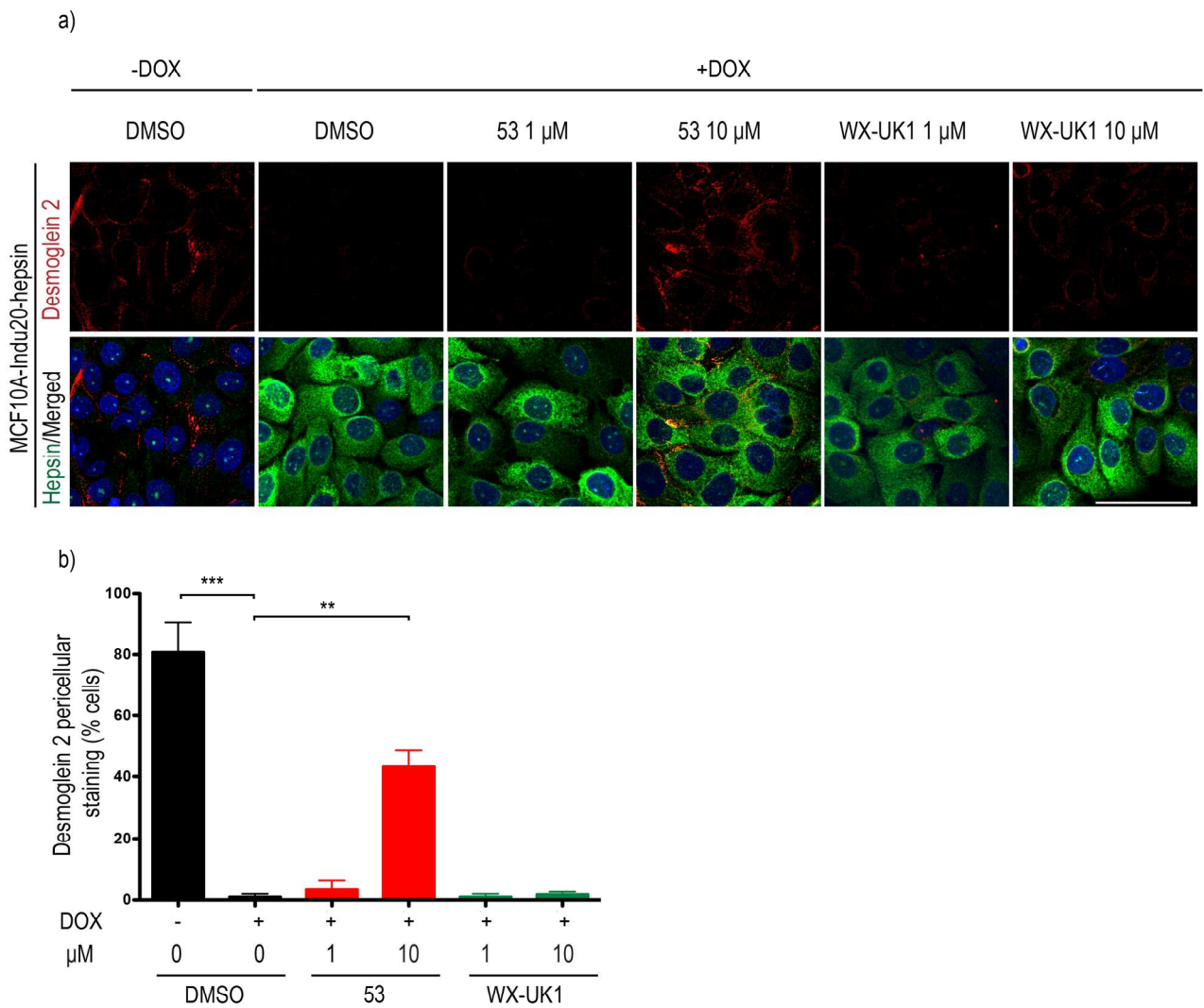


Figure 9. Inhibition of hepsin-mediated loss of desmosomal junctions by compound **53** a) Representative confocal immunofluorescence microscopy images of MCF10A-Indu20-hepsin cells with hepsin induced in the presence of indicated compounds. Note the rescue of pericellular

1 staining of desmoglein 2 by compound **53**. MCF10A-Indu20-hepsin cells were pre-treated with 1
2
3 and 10 μ M **53**, WX-UK1 or DMSO for 30 min followed by the induction of hepsin with 100
4
5
6 ng/mL Dox for 6 h on a cover slip. The scale bar is 50 μ m. b) Quantification of desmosomal
7
8 integrity. Cells expressing continuous pericellular desmoglein 2 were scored positive and
9
10 discontinuous/ absent pericellular desmoglein 2 were scored negative from immunofluorescent
11
12 images. Cells were counted from 10 fields of view per treatment from three biological replicates.
13
14 Results are shown as percentages. The p-value was derived from Student's t-test. * $p < 0.05$, ** $p <$
15
16 0.01, *** $p < 0.001$.
17
18
19
20
21
22

23 CONCLUSIONS

24
25 In the present study, we generated 142 novel compounds with hepsin and uPA IC_{50} data using the
26
27 CyclOps automated synthesis-to-screen platform. The progression from the initial hit **7** to
28
29 compound **53** was accompanied by an improvement in inhibitory activity against hepsin from ~ 1
30
31 μ M to 22 nM, and selectivity over uPA was improved from 30-fold to >6000-fold. The leading
32
33 compounds also demonstrated promising selectivity towards hepsin among a broader panel of
34
35 serine proteases. In cell-based assays compound **53** was able to inhibit the dual oncogenic
36
37 functions of hepsin, inhibiting ligand induced MET activation and loss of cellular cohesion. The
38
39 superior potency and selectivity demonstrated by compound **53** over previous small molecule tools
40
41 such as WX-UK1 means that it can serve as a valuable probe to further interrogate the oncogenic
42
43 functions of hepsin in a cellular context.
44
45
46
47
48
49
50

51 EXPERIMENTAL SECTION

Chemistry. Reagents and solvents were purchased from commercial suppliers and used without further purification. ¹H NMR spectra were recorded on a Bruker 400 MHz NMR spectrometer. Chemical shifts are reported in parts per million (ppm) relative to an internal solvent reference and coupling constants are reported in Hz, with conventional abbreviations for designation of peaks: s, singlet; d, doublet; t, triplet; q, quartet; m, multiplet; br, broad. Final compounds were ≥95% purity as assessed by analytical LC-MS; further details of the methods used can be found in the supporting information.

General platform flow synthesis method. Stock solutions of the amino acid trimethylsilyl ester (0.35 M in DCM), sulfonyl chloride (0.42 M in DCM), aminoamidine (0.35 M in NMP), and HATU (0.35 M in NMP) were prepared prior to starting the flow experiment. The stock solutions (400 μL, 1.6x overfill) were manually or automatically loaded to Vapourtec loops (250 μL volume) after which the Vapourtec FlowCommander software controlled the entire experiment. The total reaction time was around 50 min including automated loading of loops. The product solution was collected manually or using a fraction collector as it eluted from reactor 2 (see Scheme 2). When integrated to the CyclOps platform, a 20 μL aliquot of the product solution was automatically captured and purified by HPLC prior to dilution and assay.

Synthesis of non-commercial compounds from Table 6 in batch mode. (*R*)-*N*-(4-Carbamimidoylphenyl)-2-cyclohexyl-2-((4-methylphenyl)sulfonamido)acetamide (33). A solution of sodium hydroxide (53 mg, 1.34 mmol) was prepared in water (3.7 mL), (*R*)-2-amino-2-cyclohexylacetic acid (100 mg, 0.64 mmol) was added and the suspension sonicated to give a clear colourless solution of the sodium salt. A solution of 4-methylbenzene-1-sulfonyl chloride (133 mg, 0.70 mmol) in acetonitrile (3 mL) was added dropwise to the salt solution and the mixture stirred overnight to give a cloudy solution. Ethyl acetate (10 mL) was added followed by 1N HCl (5 mL).

The mixture was stirred vigorously for 5 min and the organic phase separated. A further aliquot of ethyl acetate (5 mL) was added to the aqueous phase, stirred and the organic phase separated and added to the first extract. The combined organic extracts were evaporated to dryness to give the sulfonamide intermediate, which was dissolved in NMP (1 mL) and a solution of 2-(3H-[1,2,3]triazolo[4,5-b]pyridin-3-yl)-1,1,3,3-tetramethylisouronium hexafluorophosphate(V) (HATU) (242 mg, 0.64 mmol) in NMP (1 mL) added drop-wise and the mixture stirred for 10 min to give the activated ester. A solution of 4-aminobenzamidine dihydrochloride (132 mg, 0.64 mmol) was prepared in a mixture of NMP (1 mL) and DIPEA (111 μ L, 0.64 mmol). Sonication was required to completely dissolve the material. The solution of the 4-aminobenzimidamide was added to the activated ester and the solution heated at 80°C for 20 min under microwave conditions to give a clear amber solution. The crude material was purified by reverse-phase preparative HPLC, using an acidic method (0.2% TFA as additive). The product fractions were collected and evaporated to dryness in a Genevac EZ-2 centrifugal evaporator to give the product **33** as a white solid, TFA salt (42 mg, 15%). ^1H NMR (400 MHz, d_6 -DMSO) δ ppm 10.27 (br. s, 1H), 8.48 (s, 1H), 7.72 (d, $J=8.8$ Hz, 2H), 7.63 (d, $J=8.4$ Hz, 2H), 7.52 (d, $J=8.8$ Hz, 2H), 7.18 (d, $J=8.4$ Hz, 2H), 3.64 (d, $J=8.4$ Hz, 1H), 2.17 (s, 3H), 1.83-1.75 (m, 1H), 1.70-1.51 (m, 4H), 1.44-1.33 (m, 1H), 1.17-1.01 (m, 4H), 0.91-0.80 (m, 1H); MS m/z : 429 $[\text{M}+\text{H}]^+$.

Compounds **48**, **52** and **53** were prepared using an analogous method to compound **33**:

(*R*)-*N*-(4-Carbamimidoylphenyl)-2-cyclohexyl-2-((4-fluorophenyl)sulfonamido)acetamide

(48). White solid, formic acid salt (52 mg, 19%). ^1H NMR (400 MHz, d_6 -DMSO) δ ppm 10.43 (br. s, 1H), 8.41 (br. s, 1H), 7.83-7.79 (m, 2H), 7.73 (d, $J=8.8$ Hz, 2H), 7.56 (d, $J=8.8$ Hz, 2H), 7.28-7.22 (m, 2H), 3.68 (d, $J=8.4$ Hz, 1H), 1.82-1.74 (m, 1H), 1.69-1.53 (m, 4H), 1.43-1.36 (m, 1H), 1.16-1.03 (m, 4H), 0.93-0.83 (m, 1H); MS m/z : 433 $[\text{M}+\text{H}]^+$.

(R)-N-(4-Carbamimidoylphenyl)-2-cyclohexyl-2-((4-

(trifluoromethyl)phenyl)sulfonamido)acetamide (52). Pale yellow solid, formic acid salt (14 mg, 5%). ¹H NMR (400 MHz, d₆-DMSO) δ ppm 10.40 (br. s, 1H), 8.47 (s, 1H), 7.94 (d, *J*=8.0 Hz, 2H), 7.77 (d, *J*=8.4 Hz, 2H), 7.71 (d, *J*=8.8 Hz, 2H), 7.48 (d, *J*=8.8 Hz, 2H), 3.71 (d, *J*=8.4 Hz, 1H), 1.83-1.76 (m, 1H), 1.70-1.54 (m, 4H), 1.44-1.36 (m, 1H), 1.16-1.02 (m, 4H), 0.94-0.84 (m, 1H); MS *m/z*: 483 [M+H]⁺.

(R)-N-(4-Carbamimidoylphenyl)-2-((4-methylphenyl)sulfonamido)-2-phenylacetamide (53).

White solid, formic acid salt (21 mg, 7%). ¹H NMR (400 MHz, d₆-DMSO) δ ppm 7.70 (d, *J*=8.8 Hz, 2H), 7.57 (d, *J*=8.4 Hz, 2H), 7.48 (d, *J*=8.4 Hz, 2H), 7.40-7.36 (m, 2H), 7.28-7.18 (m, 3H), 7.13 (d, *J*=8.0 Hz, 2H), 4.97 (br. s, 1H), 2.21 (s, 3H); MS *m/z*: 423 [M+H]⁺.

ASSOCIATED CONTENT**Supporting Information**

The Supporting Information is available free of charge on the ACS Publications website at DOI: 10.1021/acs.jmedchem.xxxxxx

Experimental details for enzyme and cell-based assays, synthetic methods and flow chemistry methods, analysis and separation methods, *in vitro* ADMET methods, design algorithm (doc)

Complete SAR data set for synthesized compounds (pdf)

Reactant set used to define virtual chemical space (pdf)

Molecular formula strings associated with biological data (csv)

AUTHOR INFORMATION

Corresponding Authors

* (M.R.) E-mail: manoj.ramjee@cyclofluidic.co.uk

* (T.C.) E-mail: tim.chapman@lifearc.org

* (J.K.) E-mail: juha.klefstrom@helsinki.fi

Author Contributions

S.M.P., T.T and J.K. contributed equally to this work.

Funding Sources

Cyclofluidic Ltd is grateful for support from Innovate UK (Innovate UK is an executive non-departmental public body, sponsored by the Department for Business, Energy & Industrial Strategy), Pfizer Ltd. (Ramsgate Road, Sandwich, Kent, CT13 9NJ, UK) and UCB Pharma (208 Bath Road, Slough, Berkshire SL1 3WE, UK). This work was funded by the Academy of Finland, TEKES, HiLIFE and the Finnish Cancer Organizations; SMP was funded by the Doctoral Program in Biomedicine (DPBM) and Biomedicum Helsinki Foundation.

ACKNOWLEDGMENTS

Cyclofluidic Ltd would like to thank Dave Parry and Qixing Feng for advice and technical support. JK thanks all the members of Klefström laboratory for discussions and critical comments on the manuscript. T. Ratikainen is thanked for technical assistance. Biomedicum Imaging Unit (BIU) and Biomedicum Functional Genomics Unit (FUGU) are acknowledged for core services and technical support.

ABBREVIATIONS USED

BOUS, Best objective under-sampled; Dox, Doxycycline; HAI-1, Hepatocyte growth factor inhibitor-1; HGF, Hepatocyte growth factor; Indu20, pINDUCER20; MET, Mesenchymal Epithelial Transition Factor; pMET, PhosphoMET; pro-MSP, Macrophage stimulating protein propeptide; rHPN, Recombinant human hepsin; RON, recepteur d'origine nantais; rPro-HGF, Recombinant human HGF propeptide; TNBC, Triple negative breast cancer; uPA, Urokinase-type plasminogen activator.

REFERENCES

- (1) Somoza, J. R.; Ho, J. D.; Luong, C.; Ghate, M.; Sprengeler, P. A.; Mortara, K.; Shrader, W. D.; Sperandio, D.; Chan, H.; McGrath, M. E.; Katz, B. A. The structure of the extracellular region of human hepsin reveals a serine protease domain and a novel scavenger receptor cysteine-rich (SRCR) domain. *Structure* **2003**, *11*, 1123-1131.
- (2) Dhanasekaran, S. M.; Barrette, T. R.; Ghosh, D.; Shah, R.; Varambally, S.; Kurachi, K.; Pienta, K. J.; Rubin, M. A.; Chinnaiyan, A. M. Delineation of prognostic biomarkers in prostate cancer. *Nature* **2001**, *412*, 822-826.
- (3) Tervonen T. A.; Belitškin D.; Pant, S. M.; Englund, J. I.; Marques, E.; Ala-Hongisto, H.; Nevalaita, L.; Sihto, H.; Heikkilä, P.; Leidenius, M.; Hewitson, K.; Ramachandra, M.; Moilanen, A.; Joensuu, H.; Kovanen, P.E.; Poso, A.; Klefström, J. Deregulated hepsin protease activity confers oncogenicity by concomitantly augmenting HGF/MET signalling and disrupting epithelial cohesion. *Oncogene* **2016**, *35*, 1832-1846.
- (4) Partanen, J. I.; Tervonen, T. A.; Myllynen, M.; Lind, E.; Imai, M.; Katajisto, P.; Dijkgraaf, G. J.; Kovanen, P. E.; Mäkelä, T. P.; Werb, Z.; Klefström, J. Tumor suppressor function of liver

- kinase B1 (Lkb1) is linked to regulation of epithelial integrity. *Proc. Natl Acad. Sci. USA* **2012** *109*, E388-97.
- (5) Xing P.; Li, J. G.; Jin, F.; Zhao, T. T.; Liu, Q.; Dong, H. T.; Wei, X. L. Clinical and biological significance of hepsin overexpression in breast cancer. *J. Investig. Med.* **2011**, *59*, 803-810.
- (6) Tanimoto, H.; Yan, Y.; Clarke, J.; Korourian, S.; Shigemasa, K.; Parmley, T. H.; Parham, G. P.; O'Brien, T. J. Hepsin, a cell surface serine protease identified in hepatoma cells, is overexpressed in ovarian cancer. *Cancer Res.* **1997**, *57*, 2884-2887.
- (7) Betsunoh, H.; Mukai, S.; Akiyama, Y.; Fukushima, T.; Minamiguchi, N.; Hasui, Y.; Osada, Y.; Kataoka, H. Clinical relevance of hepsin and hepatocyte growth factor activator inhibitor type 2 expression in renal cell carcinoma. *Cancer Sci.* **2007**, *98*, 491-498.
- (8) Miao, J.; Mu, D.; Ergel, B.; Singavarapu, R.; Duan, Z.; Powers, S.; Oliva, E.; Orsulic, S. Hepsin colocalizes with desmosomes and induces progression of ovarian cancer in a mouse model. *Int. J. Cancer.* **2008**, *123*, 2041-2047.
- (9) Klezovitch, O.; Chevillet, J.; Mirosevich, J.; Roberts, R. L.; Matusik, R. J.; Vasioukhin, V. Hepsin promotes prostate cancer progression and metastasis. *Cancer Cell* **2004**, *6*, 185-195.
- (10) Xuan, J. A.; Schneider, D.; Toy, P.; Lin, R.; Newton, A.; Zhu, Y.; Finster, S.; Vogel, D.; Mintzer, B.; Dinter, H.; Light, D.; Parry, R.; Polokoff, M.; Whitlow, M.; Wu, Q.; Parry, G. Antibodies neutralizing hepsin protease activity do not impact cell growth but inhibit invasion of prostate and ovarian tumor cells in culture. *Cancer Res.* **2006**, *66*, 3611-3619.
- (11) Goswami, R.; Wohlfahrt, G.; Törmäkangas, O.; Moilanen, A.; Lakshminarasimhan, A.; Nagaraj, J.; Arumugam, K. N.; Mukherjee, S.; Chacko, A. R.; Krishnamurthy, N. R.; Jaleel, M.; Palakurthy, R. K.; Samiulla, D. S.; Ramachandra, M. Structure-guided discovery of 2-

- aryl/pyridin-2-yl-1H-indole derivatives as potent and selective hepsin inhibitors. *Bioorg. Med. Chem. Lett.* **2015**, *25*, 5309-5314.
- (12) Franco, F. M.; Jones, D. E.; Harris, P. K. W.; Han, Z.; Wildman, S. A.; Jarvis, C. M.; Janetka, J. W. Structure-based discovery of small molecule hepsin and HGFA protease inhibitors: evaluation of potency and selectivity derived from distinct binding pockets. *Bioorg. Med. Chem.* **2015**, *23*, 2328-2343.
- (13) Tang, X.; Mahajan, S. S.; Nguyen, L. T.; Béliveau, F.; Leduc, R.; Simon, J. A.; Vasioukhin, V. Targeted inhibition of cell-surface serine protease hepsin blocks prostate cancer bone metastasis. *Oncotarget* **2014**, *5*, 1352-1362.
- (14) Han, Z.; Harris, P. K.; Jones, D. E.; Chugani, R.; Kim, T.; Agarwal, M.; Shen, W.; Wildman, S. A.; Janetka, J. W. Inhibitors of HGFA, matriptase, and hepsin serine proteases: a nonkinase strategy to block cell signaling in cancer. *ACS Med. Chem. Lett.* **2014**, *5*, 1219-1224.
- (15) Koschubs, T.; Dengl, S.; Dürr, H.; Kaluza, K.; Georges, G.; Hartl, C.; Jennewein, S.; Lanzendörfer, M.; Auer, J.; Stern, A.; Huang, K. S.; Packman, K.; Gubler, U.; Kostrewa, D.; Ries, S.; Hansen, S.; Kohnert, U.; Cramer, P.; Mundigl, O. Allosteric antibody inhibition of human hepsin protease. *Biochem. J.* **2012**, *442*, 483-494.
- (16) Ganesan, R.; Zhang, Y.; Landgraf, K. E.; Lin, S. J.; Moran, P.; Kirchhofer, D. An allosteric anti-hepsin antibody derived from a constrained phage display library. *Protein Eng. Des. Sel.* **2012**, *25*, 127-133.
- (17) Herter, S.; Piper, D. E.; Aaron, W.; Gabriele, T.; Cutler, G.; Cao, P.; Bhatt, A. S.; Choe, Y.; Craik, C. S.; Walker, N.; Meininger, D.; Hoey, T.; Austin, R. J. Hepatocyte growth factor is a preferred in vitro substrate for human hepsin, a membrane-anchored serine protease implicated in prostate and ovarian cancers. *Biochem. J.* **2005**, *390*, 125-136.

- (18) Ganesan, R.; Kolumam, G. A.; Lin, S. J.; Xie, M. H.; Santell, L.; Wu, T. D.; Lazarus, R. A.; Chaudhuri, A.; Kirchhofer, D. Proteolytic activation of pro-macrophage-stimulating protein by hepsin. *Mol. Cancer Res.* **2011**, *9*, 1175-1186.
- (19) Yao, H. P.; Zhou, Y. Q.; Zhang, R.; Wang, M. H. MSP-RON signalling in cancer: pathogenesis and therapeutic potential. *Nat. Rev. Cancer* **2013**, *13*, 466-481.
- (20) Zhang, Y. W.; Vande Woude, G. F. HGF/SF-met signaling in the control of branching morphogenesis and invasion. *J. Cell Biochem.* **2003**, *88*, 408-417.
- (21) Hanahan, D.; Weinberg, R. A. Hallmarks of cancer: the next generation. *Cell* **2011**, *144*, 646-674.
- (22) Renatus, M.; Bode, W.; Huber, R.; Stürzebecher, J.; Stubbs, M. T. Structural and functional analyses of benzamidine-based inhibitors in complex with trypsin: implications for the inhibition of factor Xa, tPA, and urokinase. *J. Med. Chem.* **1998**, *41*, 5445-5456.
- (23) Stürzebecher, J.; Vieweg, H.; Steinmetzer, T.; Schweinitz, A.; Stubbs, M. T.; Renatus, M.; Wikstrom, P. 3-Amidinophenylalanine-based inhibitors of urokinase. *Bioorg. Med. Chem. Lett.* **1999**, *9*, 3147-3152.
- (24) Desai, B.; Dixon, K.; Farrant, E.; Feng, Q.; Gibson, K. R.; van Hoorn, W. P.; Mills, J.; Morgan, T.; Parry, D. M.; Ramjee, M. K.; Selway, C. N.; Tarver, G. J.; Whitlock, G.; Wright, A. G. Rapid discovery of a novel series of Abl kinase inhibitors by application of an integrated microfluidic synthesis and screening platform. *J. Med. Chem.* **2013**, *56*, 3033-3047.
- (25) Valkó, K.; Bevan, C.; Reynolds, D. Chromatographic hydrophobicity index by fast-gradient RP-HPLC: a high-throughput alternative to log P/log D. *Anal. Chem.* **1997**, *69*, 2022-2029.

- (26) Barré, O.; Dufour, A.; Eckhard, U.; Kappelhoff, R.; Béliveau, F.; Leduc, R.; Overall, C. M. Cleavage specificity analysis of six type II transmembrane serine proteases (TTSPs) using PICS with proteome-derived peptide libraries. *PLoS One* **2014**, *9*, e105984.
- (27) Stürzebecher, J.; Prasa, D.; Hauptmann, J.; Vieweg, H.; Wikström, P. Synthesis and structure-activity relationships of potent thrombin inhibitors: piperazides of 3-amidinophenylalanine. *J. Med. Chem.* **1997**, *40*, 3091-3099.
- (28) Tamura, Y.; Hirado, M.; Okamura, K.; Minato, Y.; Fujii, S. Synthetic inhibitors of trypsin, plasmin, kallikrein, thrombin, C1r, and C1 esterase. *Biochim. Biophys. Acta.* **1977**, *484*, 417-422.
- (29) Aoyama, T.; Ino, Y.; Ozeki, M.; Oda, M.; Sato, T.; Koshiyama, Y.; Suzuki, S.; Fujita, M. Pharmacological studies of FUT-175, nafamstat mesylate. I. Inhibition of protease activity in vitro and in vivo experiments. *Jpn J. Pharmacol.* **1984**, *35*, 203-227.
- (30) Ramjee, M. K.; Henderson, I. M.; McLoughlin, S. B.; Padova, A. The kinetic and structural characterization of the reaction of nafamostat with bovine pancreatic trypsin. *Thromb. Res.* **2000**, *98*, 559-569.
- (31) Stürzebecher, J.; Markwardt, F.; Vieweg, H.; Wagner, G.; Walsmann, P. Synthetic inhibitors of serine proteinases. Part 31: inhibitory effect of isomeric compounds of N α -arylsulfonylated ω -amidinophenyl- α -aminoalkylcarboxylic acid amides on trypsin, plasmin and thrombin. *Pharmazie* **1984**, *39*, 411-413.
- (32) Stürzebecher, J.; Svendsen, L.; Eichenberger, R.; Markwardt, F. A new assay for the determination of factor XII in plasma using a chromogenic substrate and a selective inhibitor of plasma kallikrein. *Thromb. Res.* **1989**, *55*, 709-715.

- (33) Ruppert, C.; Pucker, C.; Markart, P.; Schmidt, R.; Grimminger, F.; Seeger, W.; Stürzebecher, J.; Gunther, A. Selective inhibition of large-to-small surfactant aggregate conversion by serine protease inhibitors of the bis-benzamidine type. *Am. J. Respir. Cell Mol. Biol.* **2003**, *28*, 95-102.
- (34) Vieweg, H.; Wagner, G. Synthesis of α -(arylsulfonylamino)- ω -phenyl-alkylcarboxylic acid 3- and 4-amidinoanilides. *Pharmazie* **1983**, *38*, 818-820.
- (35) For details of the flow chemistry system see www.vapourtec.com [Accessed on Apr 12, 2018].
- (36) Birchmeier, C.; Birchmeier, W.; Gherardi, E.; Vande Woude, G. F. Met, metastasis, motility and more. *Nat. Rev. Mol. Cell Biol.* **2003**, *4*, 915-925.
- (37) Kirchhofer, D.; Peek, M.; Lipari, M. T.; Billeci, K.; Fan, B.; Moran P. Hepsin activates pro-hepatocyte growth factor and is inhibited by hepatocyte growth factor activator inhibitor-1B (HAI-1B) and HAI-2. *FEBS Lett.* **2005**, *579*, 1945-1950.
- (38) Gherardi, E.; Birchmeier, W.; Birchmeier, C.; Vande Woude, G. Targeting MET in cancer: rationale and progress. *Nat. Rev. Cancer.* **2012**, *12*, 89-103.
- (39) Wilson, T. R.; Fridlyand, J.; Yan, Y.; Penuel, E.; Burton, L.; Chan, E.; Peng, J.; Lin, E.; Wang, Y.; Sosman, J.; Ribas, A.; Li, J.; Moffat, J.; Sutherlin, D. P.; Koeppen, H.; Merchant, M.; Neve, R.; Settleman, J. Widespread potential for growth-factor-driven resistance to anticancer kinase inhibitors. *Nature* **2012**, *487*, 505-509.

Table of Contents Graphic

